Centrum voor Wiskunde en Informatica

REPORT*RAPPORT*

MAS

Modelling, Analysis and Simulation

Modelling, Analysis and Simulation

A Runge-Kutta discontinuous-Galerkin level-set method for unsteady compressible two-fluid flow

J. Naber, B. koren

REPORT MAS-E0704 FEBRUARY 2007

Centrum voor Wiskunde en Informatica (CWI) is the national research institute for Mathematics and Computer Science. It is sponsored by the Netherlands Organisation for Scientific Research (NWO).
CWI is a founding member of ERCIM, the European Research Consortium for Informatics and Mathematics.

CWI's research has a theme-oriented structure and is grouped into four clusters. Listed below are the names of the clusters and in parentheses their acronyms.

Probability, Networks and Algorithms (PNA)

Software Engineering (SEN)

Modelling, Analysis and Simulation (MAS)

Information Systems (INS)

P.O. Box 94079, 1090 GB Amsterdam (NL)
Kruislaan 413, 1098 SJ Amsterdam (NL)
Telephone +31 20 592 9333
Telefax +31 20 592 4199

ISSN 1386-3703

A Runge-Kutta discontinuous-Galerkin level-set method for unsteady compressible two-fluid flow

ABSTRACT
In this work a numerical method for the solution of the two-dimensional Euler equations describing unsteady compressible two-fluid flow is presented. The method is based on the combination of a Runge-Kutta discontinuous Galerkin discretization of the Euler equations and a level-set method for the treatment of the two-fluid interface. The corresponding level-set equation is used in its advective form which, as opposed to the frequently used conservative form, does not generate an erroneous off-set in the interface location. A simple fix is applied to prevent the solution from becoming oscillatory near the two-fluid interface. Application of this fix requires the development of a special two-fluid slope limiter for the discontinuous Galerkin method. Numerical results show the competence of the developed method.

2000 Mathematics Subject Classification: 65M60, 76T10, 76T15
Keywords and Phrases: two-fluid flow; level-set method; Discontinuous Galerkin; slope limiters

European Conference on Computational Fluid Dynamics
ECCOMAS CFD 2006
P. Wesseling, E. Oñate and J. Périaux (Eds)

A RUNGE-KUTTA DISCONTINUOUS-GALERKIN LEVEL-SET METHOD FOR UNSTEADY COMPRESSIBLE TWO-FLUID FLOW

Jorick Naber* **and Barry Koren†**

*CWI,
P.O. Box 94079, 1090 GB Amsterdam, The Netherlands
e-mail: jorick.naber@cwi.nl

†CWI and Delft University of Technology, Faculty of Aerospace Engineering,
P.O. Box 5058, 2600 GB Delft, The Netherlands
e-mail: b.koren@tudelft.nl

Key words: Two-Fluid Flow, Level-Set Method, Discontinuous-Galerkin, Slope Limiters

Abstract. *In this work a numerical method for the solution of the two-dimensional Euler equations describing unsteady compressible two-fluid flow is presented. The method is based on the combination of a Runge-Kutta discontinuous Galerkin discretization of the Euler equations and a level-set method for the treatment of the two-fluid interface. The corresponding level-set equation is used in its advective form which, as opposed to the frequently used conservative form, does not generate an erroneous off-set in the interface location. A simple fix is applied to prevent the solution from becoming oscillatory near the two-fluid interface. Application of this fix requires the development of a special two-fluid slope limiter for the discontinuous Galerkin method. Numerical results show the competence of the developed method.*

1 INTRODUCTION

Two-fluid flows, where two non-mixing fluids are separated by a sharp interface, find many applications in both engineering and physics. The present work concerns the development of a highly accurate numerical solver for the simulation of compressible, unsteady, inviscid two-fluid flows described by the two-dimensional Euler equations of gas dynamics.

The two-fluid flow solver that is developed in this work is based on the *level-set* (LS) method. This method, developed in 1964 by Markstein [14] and further extended by Osher *et al.* [15, 17], describes the evolution of the interface in a two-fluid flow and as such is able to distinguish between both fluids. The LS method has been applied to two-fluid flow simulation regularly and corresponding results have shown its competence. The novelty of the solver presented here is the application of a highly accurate *Runge-Kutta discontinuous Galerkin* (RKDG) method for the temporal and spatial discretization of

the governing equations. Here the method developed by Cockburn, Shu *et al.* [2, 3, 4, 5] is followed. The possibility of obtaining very high orders of accuracy and the relatively easy implementation of mesh and order of accuracy refinement (*hp*-refinement) makes the RKDG method an attractive method for solving fluid-flow problems. Applying a RKDG discretization to a two-fluid flow solver based on the LS method, combines the accuracy of the former with the efficiency and easy implementation of the latter, and as such results in an attractive numerical solver for two-fluid flows.

In section 2 the flow model is presented. The numerical method is treated in section 3, followed by a discussion of fixes for the *pressure oscillations* in section 4. A simple fix by Abgrall and Karni [1] is applied to prevent the solution from becoming oscillatory near the two-fluid interface. Application of this fix requires the development of a special two-fluid slope limiter for the RKDG method. In section 5 numerical results of several one- and two-dimensional problems show the competence of the developed method. As a showcase for the present method's capabilities a supersonic, two-fluid jet flow is considered.

2 TWO-FLUID FLOW MODEL

2.1 Euler equations

The Euler equations form a system of nonlinear hyperbolic conservation laws representing conservation of mass, momentum and energy. For the two-dimensional case they read:

$$\frac{\partial \boldsymbol{q}}{\partial t} + \nabla \cdot \boldsymbol{F}(\boldsymbol{q}) = \frac{\partial \boldsymbol{q}}{\partial t} + \frac{\partial \boldsymbol{f}(\boldsymbol{q})}{\partial x} + \frac{\partial \boldsymbol{g}(\boldsymbol{q})}{\partial y} = \boldsymbol{0}, \tag{1}$$

where the conservative state vector $\boldsymbol{q}$ and the flux vectors $\boldsymbol{f}$ and $\boldsymbol{g}$ are given by:

$$\boldsymbol{q} = \begin{pmatrix} \rho \\ \rho u \\ \rho v \\ \rho E \end{pmatrix} \quad , \quad \boldsymbol{f} = \begin{pmatrix} \rho u \\ p + \rho u^2 \\ \rho uv \\ \rho uH \end{pmatrix} \quad \text{and} \quad \boldsymbol{g} = \begin{pmatrix} \rho v \\ \rho uv \\ p + \rho v^2 \\ \rho vH \end{pmatrix}. \tag{2}$$

In here, ρ is the density of the fluid, u and v the velocity components, p the pressure, E the total energy and H the total enthalpy. The total energy can be written as a combination of the internal energy e and the kinetic energy:

$$E = e + \frac{1}{2}(u^2 + v^2). \tag{3}$$

The total enthalpy H is defined as:

$$H = E + \frac{p}{\rho}. \tag{4}$$

We restrict ourselves to perfect gases. This allows for the use of an equation of state that explicitly relates the internal energy e and the primitive thermodynamic variables (density ρ and pressure p):

$$p = \rho e \left(\gamma - 1\right), \tag{5}$$

with γ the ratio of specific heats. In the two-fluid flow model used here this ratio of specific heats is what distinguishes one fluid from the other. Hence, when treating a two-fluid flow, both fluids are characterized by their own specific value for γ. Two-fluid flow simulation thus means solving the Euler equations with a correct distribution of the ratio of specific heats.

2.2 Level-set method

The evolution of the two-fluid interface, and thus of the distribution of the ratio of specific heats γ, is described by the level-set (LS) method. It makes use of a signed distance function φ – the LS function – to implicitly describe the interface location. The LS function labels every discrete point in the flow domain with a value representing the shortest distance to the interface and a sign indicating in which of the two fluids the discrete point is located. As such the zero LS contour represents the interface.

2.2.1 Level-set equation

The LS function φ is a scalar parameter that is advected by the flow with the local flow velocity without influencing the flow itself; a passive scalar. The well-known advection equation can be used to describe its motion:

$$\frac{\partial \varphi}{\partial t} + \boldsymbol{V} \cdot \nabla \varphi = \frac{\partial \varphi}{\partial t} + u\frac{\partial \varphi}{\partial x} + v\frac{\partial \varphi}{\partial y} = 0. \tag{6}$$

Besides the advective form of the LS equation there exists a second frequently used form; the conservative form. Multiplying equation (6) with the density ρ and adding it to the equation for conservation of mass multiplied with the LS function φ, results in:

$$\frac{\partial \rho\varphi}{\partial t} + \nabla \cdot \rho\boldsymbol{V}\varphi = \frac{\partial \rho\varphi}{\partial t} + \frac{\partial \rho u\varphi}{\partial x} + \frac{\partial \rho v\varphi}{\partial y} = 0. \tag{7}$$

This conservation law for the LS function can be added to the Euler equations as an additional equation. As such the LS equation can be solved with exactly the same numerical techniques as the original Euler equations. Although this conservation approach seems preferable above a separate treatment of the LS equation, it was shown in, e.g., [10] that it is not.

Numerically solving for the LS function using the conservative approach introduces numerical errors which lead to an unphysical off-set of the LS function and thus a wrong location of the interface. These errors do not occur when the advective approach is taken, as can be seen from the numerical results of a simple one-dimensional test problem – the translating interface problem – in figure 1. This problem treats an interface separating

two fluids with initial conditions $(\rho, u, p, \gamma)_L = (1000.0, 1.0, 1.0, 1.4)$ and $(\rho, u, p, \gamma)_R = (1.0, 1.0, 1.0, 1.6)$, which moves from its initial position $x = 0$ with a constant velocity to the right.

Clearly visible in the left plot of the distribution of the ratio of specific heats γ is the difference between the location of the numerical and the exact interface. The location of the numerical interface has a clear off-set to the right compared to the exact interface location. This off-set leads to the use of the wrong fluid properties near the interface and thus in an incorrect calculation of the flow solution (density, velocity and pressure). In the case of the advective approach this off-set is not present as can be seen in the right plot of figure 1.

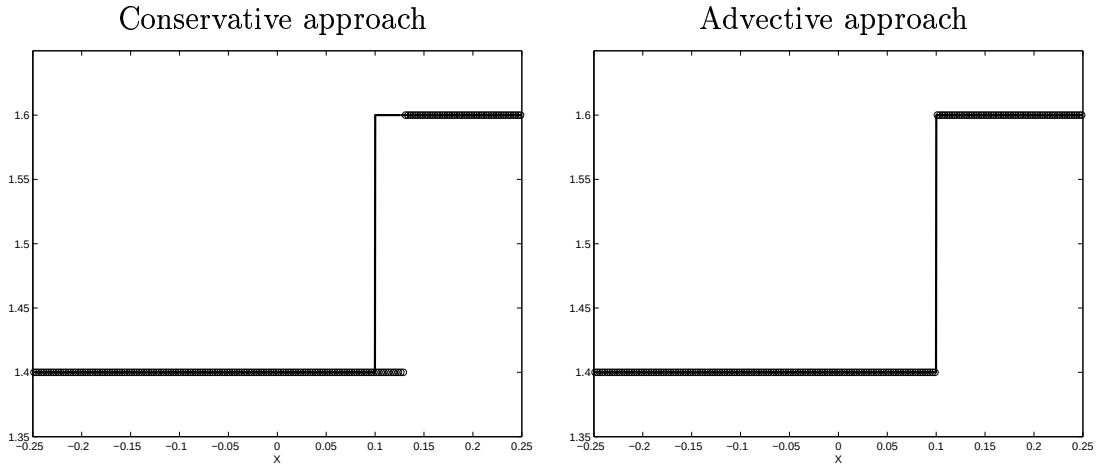

Figure 1: 1D translating interface problem. Ratio of specific heats γ at $t = 0.1$. The grid has 200 cells and $\Delta t/\Delta x = 0.5$. Solid lines are exact solutions, markers are numerical solutions. *Left:* Conservative approach. *Right:* Advective approach.

2.2.2 Redistancing

The advection equation for the LS function transports the values of φ with the local velocity. In the general case of a non-uniform velocity field this results in the advection of the different LS values such that the signed distance function is not preserved. Only the interface, having $\varphi = 0$, remains correct because it is not measured relative to another point, all non-zero values for φ are distorted as the LS function is changed in time. To assure that the LS function remains a true distance function at all time it is therefore necessary to *redistance* the LS function after each time step.

A commonly used method for the redistancing of the LS function is the so-called *PDE approach* presented by Sussman *et al.* [19, 20]. For this the following differential equation is solved until its steady state is reached:

$$\frac{\partial \varphi}{\partial \tau} = S\left(\varphi_{\tau=0}\right)\left(1 - |\nabla \varphi|\right), \tag{8}$$

where τ is an artificial time scale only used within the redistancing procedure and $S\left(\varphi_{\tau=0}\right)$ the sign function of φ_0. A steady state, i.e. $\frac{\partial \varphi}{\partial \tau} = 0$, is reached when the gradient of φ is equal to one. When this is the case, the LS function has been transformed to a true signed distance function again.

3 NUMERICAL METHOD

The choice for the advective LS approach allows for a separate numerical treatment of the Euler equations and the LS equation. Given an initial distribution of the ratio of specific heats γ, the Euler equations can be solved for the flow variables. The resulting velocity field $\boldsymbol{V}$ can then be used to solve the LS equation for a new LS distribution, and thus a new distribution of the ratio of specific heats. The discretization methods for both solution steps will be discussed here.

3.1 RKDG discretization of Euler equations

For the discretization of the Euler equations the RKDG method by Cockburn, Shu *et al.* [2, 3, 4, 5] is used. This discretization method combines the well-known explicit Runge-Kutta (RK) time-marching method with a discontinuous-Galerkin (DG) finite-element discretization of the Euler equations. A slope limiter is introduced to prevent the solution from becoming oscillatory near flow discontinuities.

3.1.1 Space discretization

The spatial grid is chosen to consist of uniform rectangular cells. Within these cells an approximate solution vector $\boldsymbol{q}_h$ is defined, which is allowed to be discontinuous over the cell-faces. Following the work of Cockburn and Shu the approximate solution in a cell $E_{i,j}$ is written as a combination of unknowns and basis functions of the order p:

$$\boldsymbol{q}_h\left(x, y, t\right) = \sum_{k,l=0}^{p} \boldsymbol{q}_{i,j}^{(k,l)}\left(t\right) \phi_i^{(k)}\left(x\right) \psi_j^{(l)}\left(y\right), \qquad \forall x, y \in E_{i,j}, \tag{9}$$

where $\phi_i^{(k)}$ and $\psi_j^{(l)}$ are the basis functions in x- and y-direction, respectively and $\boldsymbol{q}_{i,j}^{(k,l)}$ the *degrees of freedom* or *unknowns* of the approximate solution. For the basis functions one-dimensional orthogonal *Legendre polynomials* are used, which read for the x-direction:

$$\phi_i^{(0)} = 1, \quad \phi_i^{(1)} = \frac{x - x_i}{\Delta x}, \quad \phi_i^{(2)} = \frac{\left(x - x_i\right)^2}{\Delta x^2} - \frac{1}{12}, \quad \ldots. \tag{10}$$

The basis functions for the y-direction are similar. Substitution of the expression for $\boldsymbol{q}_h$ into the weak formulation of the Euler equations results in a system of equations for the

unknowns $\boldsymbol{q}_{i,j}^{(k,l)}$. The integral terms in these equations are approximated using standard Gaussian quadrature rules with $p+1$ integration points. Solving the resulting system for the unknowns requires the calculation of cell-face fluxes. For this Roe's approximate Riemann solver is used. It was shown by Cockburn and Shu that the resulting DG method is formally $\mathcal{O}(\Delta x^{p+1})$ accurate for systems of hyperbolic conservations laws.

3.1.2 Time discretization

The semi-discrete system of equations following from the DG discretization can be written as a system of ODE's, $\frac{d}{dt}\boldsymbol{q}_h = \boldsymbol{L}_h(\boldsymbol{q}_h)$. For the time discretization of this system of equations an explicit RK method is used. In order to have a time discretization that has the same order of accuracy as the spatial discretization, a RK scheme with $p+1$ intermediate stages is chosen. The resulting scheme that marches the approximate solution from time level t^n to $t^{n+1} = t^n + \Delta t$ reads:

$$\begin{aligned} \boldsymbol{q}_h^{(0)} &= \boldsymbol{q}_h^n, \\ \boldsymbol{q}_h^{(k)} &= \sum_{m=0}^{k-1} \left\{ \alpha_{km} \boldsymbol{q}_h^{(m)} + \beta_{km} \Delta t^{(m)} \boldsymbol{L}_h \left(\boldsymbol{q}_h^{(m)} \right) \right\}, \quad k = 1, \ldots, p+1, \\ \boldsymbol{q}_h^{n+1} &= \boldsymbol{q}_h^{(p+1)}. \end{aligned} \tag{11}$$

It can be shown that for the scheme described above to be numerically stable the following condition has to be satisfied:

$$c\frac{\Delta t}{\Delta x} \leq \frac{1}{2p+1}, \tag{12}$$

where c is the maximum wave speed present in the problem treated.

3.1.3 Slope limiting

To avoid spurious solution oscillations, we need to introduce a nonlinear dissipative mechanism into our numerical scheme. Following the work of Van Leer [12, 13], Cockburn and others have applied the so-called *local projection limiting* or *slope limiting* technique to the DG method. Their TVDM slope limiter ensures that the solution remains monotone without degrading the accuracy of the numerical method to first-order accuracy, which is what a slope limiter normally tends to do locally. The limiter used here is based on the one-dimensional limiter developed by Cockburn and Shu [2]. In order to implement slope limiting the approximate solution is replaced by a limited version (indicated by the $*$):

$$\boldsymbol{q}_h^*(x,y,t) = \boldsymbol{q}_{i,j}^{(0,0)} + \frac{(x-x_i)}{\Delta x}\boldsymbol{q}_{i,j}^{(1,0)*} + \frac{(y-y_j)}{\Delta y}\boldsymbol{q}_{i,j}^{(0,1)*} + \cdots. \tag{13}$$

Here the unknowns $\boldsymbol{q}_{i,j}^{(1,0)}$ and $\boldsymbol{q}_{i,j}^{(0,1)}$ are interpreted as the first-order derivatives or slopes of the approximate solution, which are replaced by the limited versions:

$$\boldsymbol{q}_{i,j}^{(1,0)*} = \text{minmod}\left(\boldsymbol{q}_{i,j}^{(1,0)}, \frac{\boldsymbol{q}_{i+1,j}^{(0,0)} - \boldsymbol{q}_{i,j}^{(0,0)}}{\lambda}, \frac{\boldsymbol{q}_{i,j}^{(0,0)} - \boldsymbol{q}_{i-1,j}^{(0,0)}}{\lambda}\right), \tag{14}$$

$$\boldsymbol{q}_{i,j}^{(0,1)*} = \text{minmod}\left(\boldsymbol{q}_{i,j}^{(0,1)}, \frac{\boldsymbol{q}_{i,j+1}^{(0,0)} - \boldsymbol{q}_{i,j}^{(0,0)}}{\lambda}, \frac{\boldsymbol{q}_{i,j}^{(0,0)} - \boldsymbol{q}_{i,j-1}^{(0,0)}}{\lambda}\right). \tag{15}$$

When λ is set equal to one this is the slope limiter used in the MUSCL schemes of Van Leer [12, 13]. A less restrictive limiter is obtained when $\lambda = \frac{1}{2}$ is used.

It is assumed that spurious oscillations are only present in the *linear* part of $\boldsymbol{q}_h$. So if the slope limiter decides to limit, the higher-order parts of the approximate solution $\boldsymbol{q}_h$ are neglected.

3.2 Discretization of LS equation

For the discretization of the LS advection equation many techniques are available. Here a finite-volume discretization based on the slope limiter by Koren [11] is used for the space discretization. Marching in time is done using an explicit fourth-order Runge-Kutta method. Discretization of the redistancing equation (8) is rather straightforward. It is explained in [16].

4 PRESSURE OSCILLATIONS

One of the major problems of conservative methods for compressible two-fluid flows is the occurrence of *spurious pressure oscillations*. Due to the inconsistency of conservative schemes near the interface large errors occur that do not disappear with decreasing mesh-size. These oscillations have been the subject of extensive research for the past ten years, leading to several adequate fixes, among which the *ghost-fluid method* by Fedkiw *et al.* [6] and the fixes by Karni [8, 9]. Here a locally non-conservative fix, proposed by Abgrall and Karni [1], is used. The approach is comparable to the ghost-fluid method but is simpler to implement and requires less computational power.

4.1 Simple fix

Abgrall and Karni [1] showed in 1D that for a two-fluid model based on a jump in the distribution of the ratio of specific heats γ, the numerical solution remains oscillation-free only in the special case that:

$$\gamma_L = \gamma_R \qquad \text{and} \qquad \gamma_i^{n+1} = \gamma_i^n,$$

where γ_L and γ_R are the ratio of specific heats of the fluids left and right of the interface respectively, and γ_i^{n+1} and γ_i^n the ratio of specific heats in cell i at discrete time levels $n+1$ and n. Thus, spurious pressure oscillations are prevented when there is locally no jump in the distribution of the ratio of specific heats ($\gamma_L = \gamma_R$) and when the interface

is temporarily *frozen* during the update of the ratio of specific heats ($\gamma_i^{n+1} = \gamma_i^n$). The simple fix makes that both conditions are satisfied.

The first of these conditions is satisfied by using only one value of γ in the calculation of the cell-face fluxes. Thus instead of a flux update that uses information of both fluids (when an interface is present), the method is allowed to use only information from one fluid. The fluxes are made *blind* for any other fluid than the one present in the cell the flux updates. Although this implies that conservation is locally abandoned – the flux updating the cell with γ_L is no longer equal to the flux updating the cell with γ_R (see figure 2) – it is a necessary condition for an oscillation-free solution.

The second part of the simple fix consists of temporarily freezing the ratio of specific heats. Conversion of the total energy ρE to the pressure p, which is a necessary step in the solution of the Euler equations, is done using an old or *frozen* value of γ, i.e. $\gamma_i^{n+1} = \gamma_i^n$. This makes that the pressure distribution, and consequently the velocity and density distributions, produce no spurious oscillations.

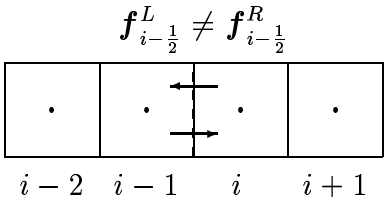

Figure 2: The simple fix applied to grid cell i containing an interface (dotted line) separating two fluids with $\gamma_L \neq \gamma_R$. The simple fix locally abandons conservation by using two different numerical fluxes $\boldsymbol{f}$ at the cell interface separating both fluids.

The resulting simple fix effectively prevents spurious oscillations from occurring when used in a finite-volume setting for two-fluid problems. When applied to the DG method however, it is not sufficient to solely adapt the cell-face fluxes and freeze the ratio of specific heats during the update step. This because in the DG method the complete approximate solution is limited, instead of only the solution values used for the flux calculation as is the case for general finite-volume solvers. Since the limiter *looks out of the cell* and is thus able to detect a possible jump in the distribution of the ratio of specific heats γ, spurious oscillations can be generated. To prevent this, the abovementioned simple fix needs to be extended to the slope limiter used in the DG method, resulting in a two-fluid slope limiter.

4.2 Two-fluid slope limiter for DG

Also in the slope limiter a fix is applied that prevents the limiter from *seeing* two different values of γ. Since the oscillations result from the equation for the total energy this fix is only applied to the approximation of the total energy ρE. The original slope limiter for the energy equation reads as follows:

$$\rho E_h^* = \rho E_{i,j}^{(0,0)} + \frac{(x-x_i)}{\Delta x}\rho E_{i,j}^{(1,0)*} + \frac{(y-y_j)}{\Delta y}\rho E_{i,j}^{(0,1)*} + \cdots, \tag{16}$$

with the limited slopes:

$$\rho E_{i,j}^{(1,0)*} = \text{minmod}\left(\rho E_{i,j}^{(1,0)}, \frac{\rho E_{i+1,j}^{(0,0)} - \rho E_{i,j}^{(0,0)}}{\lambda}, \frac{\rho E_{i,j}^{(0,0)} - \rho E_{i-1,j}^{(0,0)}}{\lambda}\right), \tag{17}$$

$$\rho E_{i,j}^{(0,1)*} = \text{minmod}\left(\rho E_{i,j}^{(0,1)}, \frac{\rho E_{i,j+1}^{(0,0)} - \rho E_{i,j}^{(0,0)}}{\lambda}, \frac{\rho E_{i,j}^{(0,0)} - \rho E_{i,j-1}^{(0,0)}}{\lambda}\right). \tag{18}$$

Spurious oscillations occur when this limiter uses two different values for γ during the calculations. It is clear that only the terms $\rho E_{i-1,j}^{(0,0)}$, $\rho E_{i+1,j}^{(0,0)}$, $\rho E_{i,j-1}^{(0,0)}$ and $\rho E_{i,j+1}^{(0,0)}$ can be responsible for such a situation. Whenever an interface is present in the cells under consideration, such that for example $\gamma_{i,j} \neq \gamma_{i-1,j}$, these expressions will introduce different values of γ into the limiter, resulting in the spurious oscillations..

To prevent the solution from becoming oscillatory we require the limiter to use only $\gamma_{i,j}$ instead of $\gamma_{i\pm1,j}$. Therefore we replace the original expressions for the total energy in the neighboring cells with *fixed* expressions: $\widehat{\rho E}_{i\pm1,j}^{(0,0)} = \rho E_{i\pm1,j}^{(0,0)}(\gamma_{i,j})$, and the same in the y-direction. Given the expression for the total energy $\rho E = \frac{p}{\gamma-1} + \frac{1}{2}\rho(u^2+v^2)$ these expressions for the x-direction can be written as follows:

$$\widehat{\rho E}_{i-1,j}^{(0,0)} = \rho E_{i-1,j}^{(0,0)} + p_{i-1,j}^{(0,0)}\left[\left(\frac{1}{\gamma-1}\right)_{i,j} - \left(\frac{1}{\gamma-1}\right)_{i-1,j}\right], \tag{19}$$

$$\widehat{\rho E}_{i+1,j}^{(0,0)} = \rho E_{i+1,j}^{(0,0)} + p_{i+1,j}^{(0,0)}\left[\left(\frac{1}{\gamma-1}\right)_{i,j} - \left(\frac{1}{\gamma-1}\right)_{i+1,j}\right], \tag{20}$$

where $p_{i,j}^{(0,0)}$ is the mean pressure that can easily be calculated from the mean total energy.

It is clear that, similar to the simple fix applied in the flux calculation and the pressure update, the *fixed* slope limiter developed above also introduces numerical errors that are not present in the original single-fluid slope limiter. From (19) and (20) it follows that the difference between using the *correct* value of γ and the *fixed* value of γ is equal to:

$$\widehat{\rho E}_{i\pm1,j}^{(0,0)} - \rho E_{i\pm1,j}^{(0,0)} = p_{i\pm1,j}^{(0,0)}\Delta\left(\frac{1}{\gamma-1}\right), \tag{21}$$

which is similar to the expressions found for the original simple fix. The errors introduced by the fix can be neglected with respect to the errors made when this fix would not be applied.

5 NUMERICAL RESULTS

In this section numerical results are presented. Besides two standard problems, also a novel problem – a supersonic jet flow – is considered. Unless stated otherwise results are obtained using quadratic basis functions ($p = 2$) and the less restrictive limiter with $\lambda = \frac{1}{2}$.

5.1 Two-fluid Sod problem

The initial data for this problem are $(\rho, u, p, \gamma)_L = (1.0, 0.0, 1.0, 1.4)$ and $(\rho, u, p, \gamma)_R = (0.125, 0.0, 0.1, 1.6)$. The results are plotted in figure 3. The numerical results comply well with the exact solution. The discontinuous phenomena, i.e., the contact discontinuity and the shock wave, are in their correct locations. The shock and contact discontinuity are sharp and show no signs of undesired oscillations, indicating that the limiter performs well.

5.2 Shock-bubble interaction

The performance of the numerical solver for two-dimensional problems is tested on a problem treating the interaction of a shock moving in air and a bubble containing a different gas which is initially at rest. This problem is taken from the experiments by Haas and Sturtevant [7]. Numerical results obtained for this problem can be found in, e.g., [18, 21]. In the test to be considered the circular bubble in air contains helium. The initial conditions are given in table 1. The grid is taken equal to 400×200 cells in accordance to the simulation by Wackers [21].

	γ	ρ	u	v	p
$\text{air}_{stagnant}$	1.4	1.40000	0.00000	0.00000	1.00000
air_{moving}	1.4	1.92691	0.33361	0.00000	1.56980
helium	1.648	0.25463	0.00000	0.00000	1.00000

Table 1: Initial conditions for the 'shock-bubble interaction' test case.

In the plots of the density and the pressure (figure 4) one recognizes the characteristic wave pattern. The refracted shock, travelling faster than the incoming shock, is clearly visible. Even after having passed twice through the two-fluid interface this shock is still surprisingly sharp and in the correct location, indicating that there is no apparent loss of accuracy due to the method being locally non-conservative. The resulting two-fluid interface itself is also very sharp.

To further evaluate the results obtained with the present method the velocities of several waves are compared with known data. In table 2 the velocities of the incoming shock, the refracted shock and the interface, c_s, c_r and c_i, respectively, are given. The first is measured at the top of the computational domain, the latter two at the symmetry

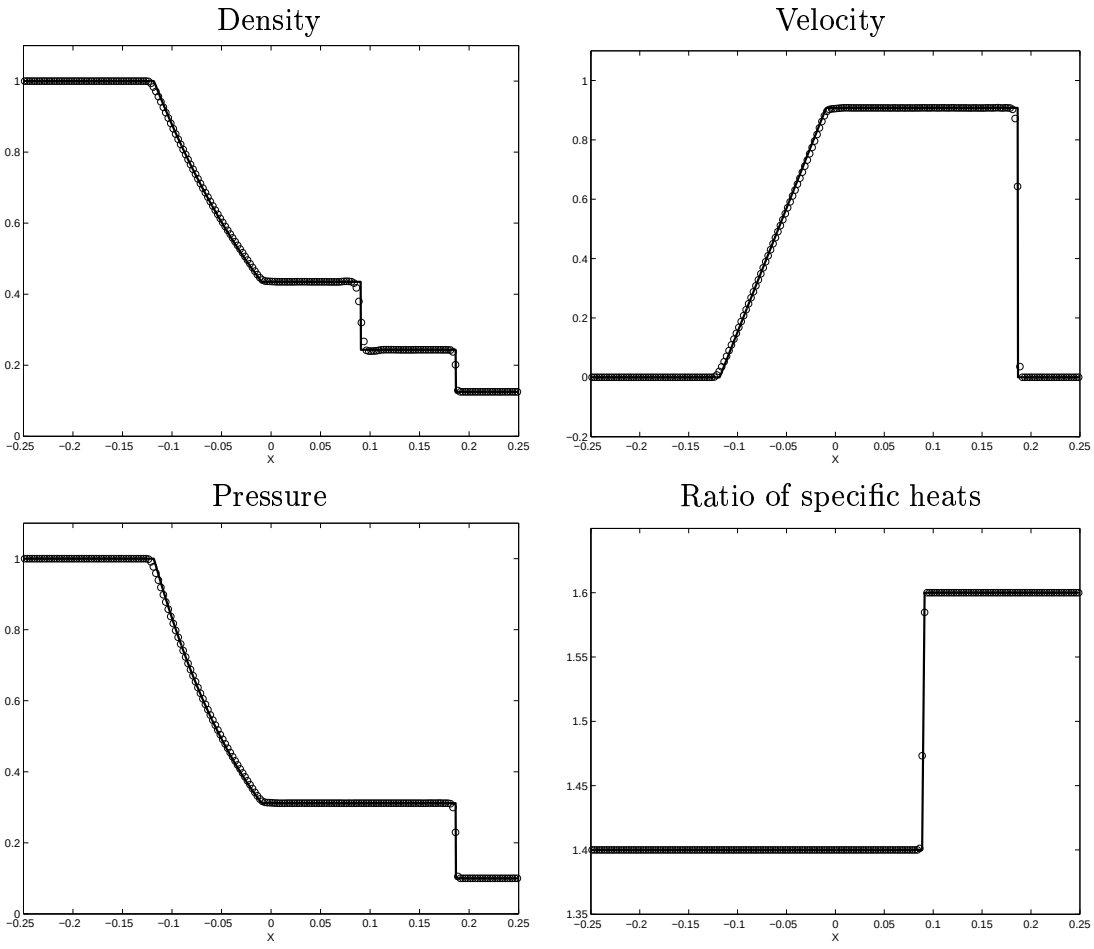

Figure 3: Results of two-fluid Sod problem. Primary variables against the x-location in the tube at $t = 0.1$. The grid consists of 200 cells. The values in cell centers are plotted. Solid line: exact solution, markers: numerical solution.

line. From the table it appears that the present method performs reasonably well. The incoming shock speed complies very well with previous results. The refracted shock speed and the interface speed lie somewhat higher than the other results.

	$c_s[m/s]$	$c_r[m/s]$	$c_i[m/s]$
Present method	419	955	181
Quirk & Karni [18]	422	943	178
Wackers & Koren [21]	419	950	173
Haas & Sturtevant [7]	410	900	170

Table 2: Wave speeds in helium-bubble test. Incoming shock speed c_s measured at the top of the domain, refracted shock speed c_r and interface speed c_i at the symmetry line.

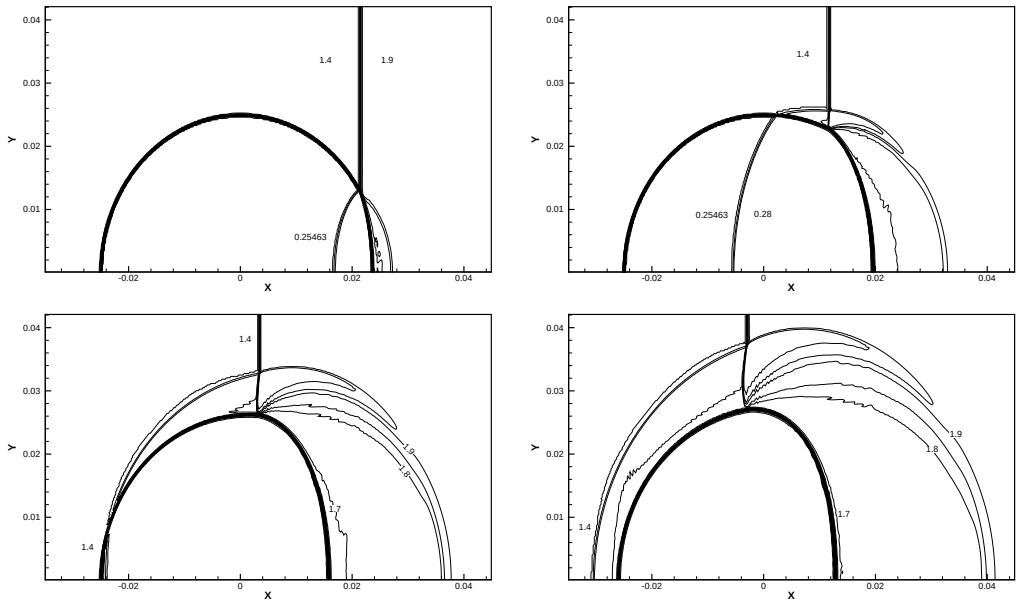

5.3 Overexpanded rocket jet

A free jet occurs when a high-velocity flow exits a nozzle into a gas, often air, producing a jet with characteristics depending on the properties of the jet and the ambient gas. Interesting situations occur when the jet exits in a gas with either a higher or a lower pressure. For a fixed nozzle geometry, the exhaust conditions of the nozzle flow will remain the same while the ambient pressure decreases with increasing height. When the jet is below its so-called *design height*, i.e., the height for which the jet at the nozzle exit and the ambient air have exactly the same pressure, the jet is called *overexpanded*. Then, the

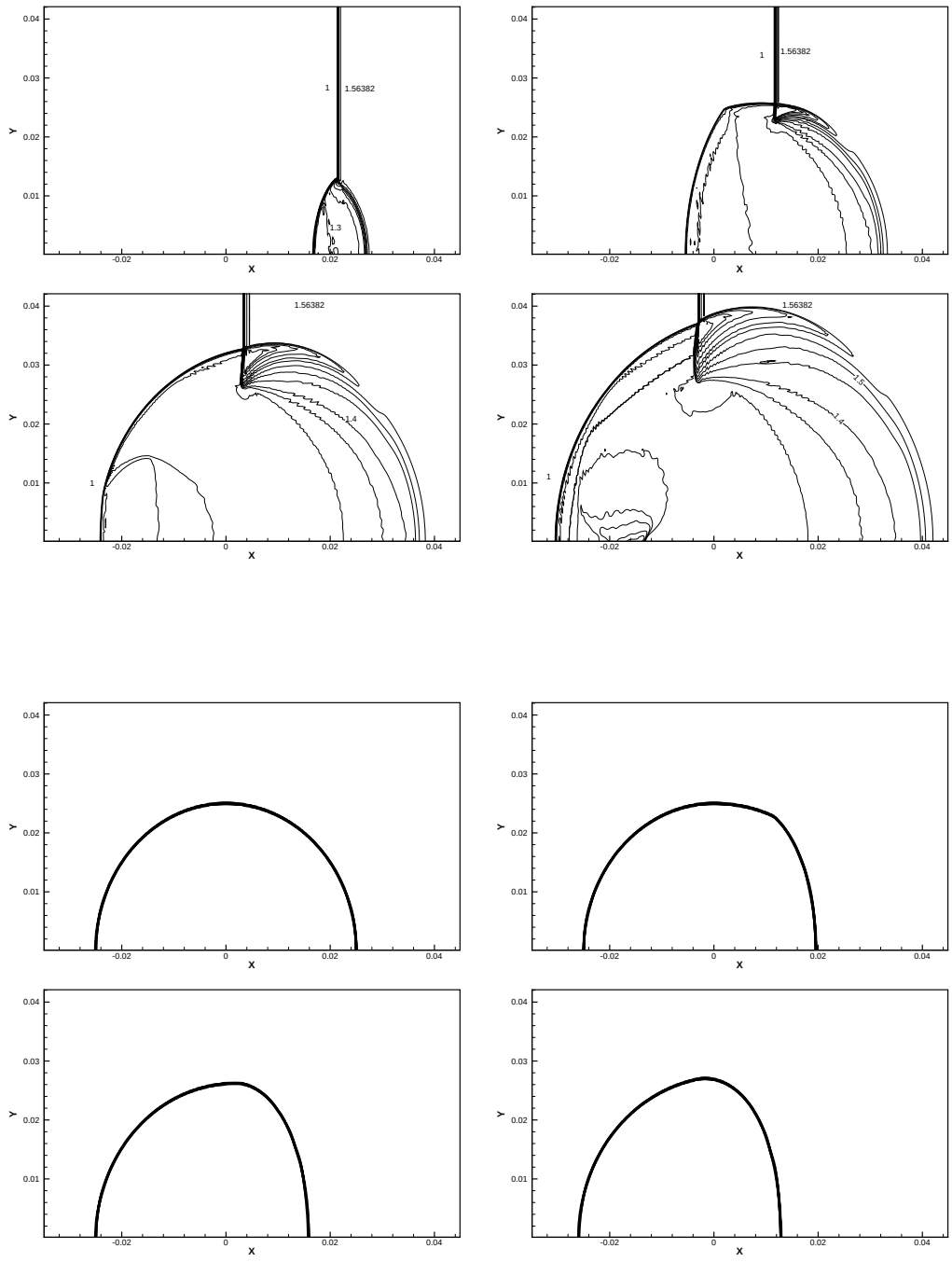

Figure 4: Shock hitting helium bubble at $t = 5 \times 10^{-3}$, $t = 13 \times 10^{-3}$, $t = 19.8 \times 10^{-3}$ and $t = 25 \times 10^{-3}$. First, second and third series: density, pressure and ratio of specific heats, respectively. The grid has 300×150 cells and $\Delta t = 0.25 \times 10^{-5}$.

exhaust pressure is lower than the ambient pressure. In case the jet is above its design height it is called *underexpanded*. In both cases the jet will deform due to the appearance of shocks and expansion fans, which adapt the jet pressure to the ambient pressure.

In our test problem, the exhaust gas is taken to be CO_2, and for the ambient gas air is used. We consider an overexpanded case. The initial thermodynamic state variables (scaled) are given in table 3. The ratio of specific heats for CO_2 is assumed to be 1.3, while that of air is 1.4. For the air, atmospheric conditions at sea level are used, which are scaled such that the speed of sound is equal to 1. The air is further assumed to flow with a supersonic speed, in the same direction as the jet. The conditions for the CO_2 are chosen such that also the jet has a speed of sound equal to 1. Note that these conditions correspond to a jet temperature of $T_{CO_2} = 1.65 T_{\text{air}}$.

	γ	ρ	u	v	p
Air (overexp.)	1.4	1.4	2.0	0.0	2.0
CO_2 (overexp.)	1.3	1.3	4.0	0.0	1.0

Table 3: Initial conditions for the supersonic free jet problem.

The numerical results for the overexpanded jet are given in figure 5. In the plots of the ratio of specific heats γ, the start-up of the jet is clearly visible. Due to the start-up bow shock, a negative pressure gradient in transverse direction is built up around the head of the jet. Hence, the head also grows wider. At later stages the outer parts of this jet head curve backwards and form the characteristic *mushroom* shape. Together with the start-up shock also the jet head moves out of the computational domain.

6 CONCLUSIONS

In this work a numerical method for the solution of the two-dimensional Euler equations describing unsteady compressible two-fluid flows has been presented. The method is based on the combination of a Runge-Kutta discontinuous Galerkin (RKDG) discretization method for the Euler equations and a level-set (LS) method for the treatment of the two-fluid interface.

Typical for conservative two-fluid flow methods is that they generate spurious oscillations near the two-fluid interface. In order to prevent these oscillations a simple fix has been applied. The first part of this fix is based on the requirement that a numerical cell can only use information from one fluid. The second part of the fix requires that during an update of the state variables only the old value of the ratio of specific heats can be used. A novel two-fluid slope limiter has also been proposed. It is based on the simple pressure fix.

Numerical tests have been performed to evaluate the performance of the present method. Shock waves and two-fluid interfaces show less numerical diffusion than results obtained

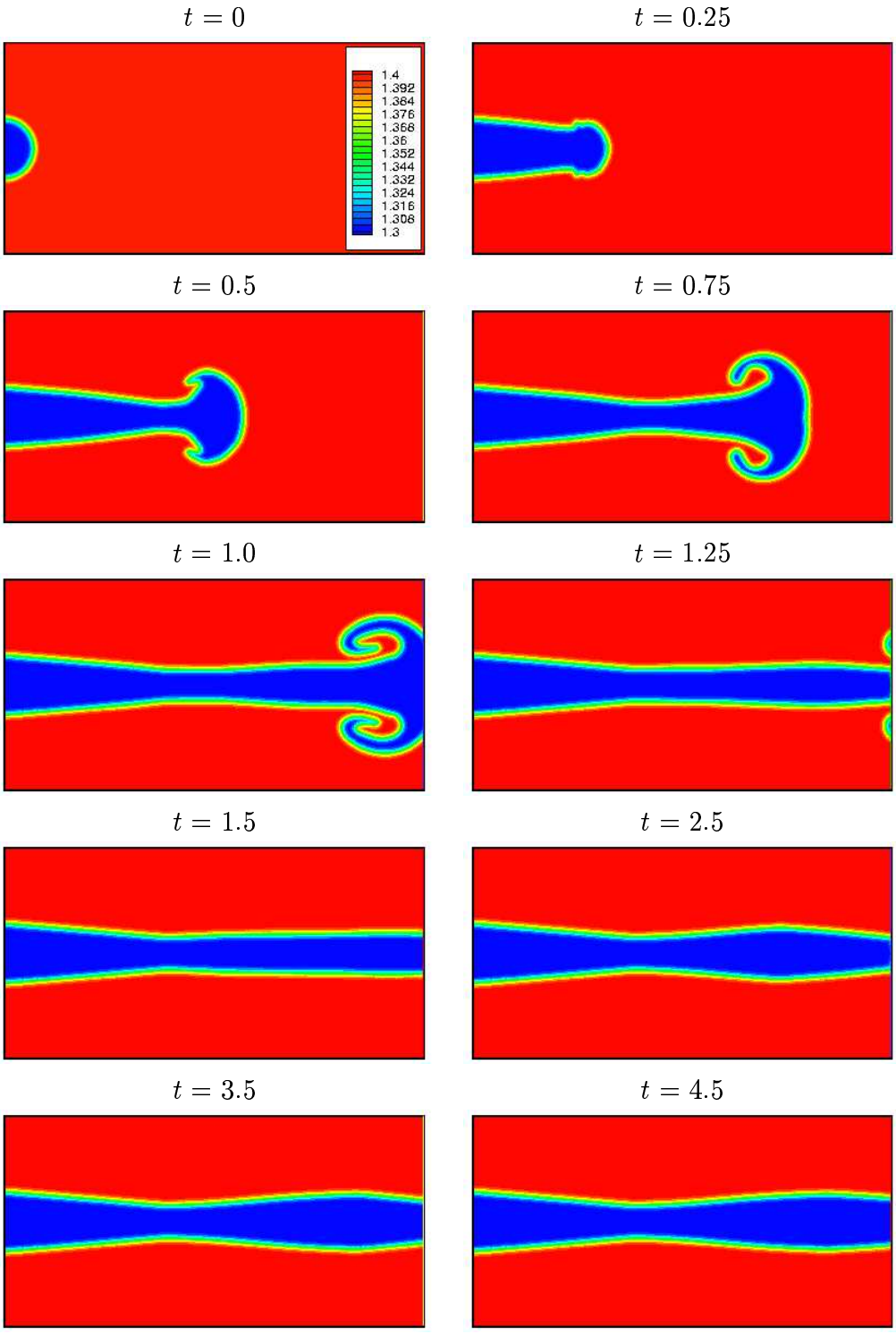
$t = 0$
1.4
1.392
1.384
1.376
1.368
1.36
1.352
1.344
1.332
1.324
1.316
1.308
1.3
$t = 0.25$
$t = 0.5$
$t = 0.75$
$t = 1.0$
$t = 1.25$
$t = 1.5$
$t = 2.5$
$t = 3.5$
$t = 4.5$

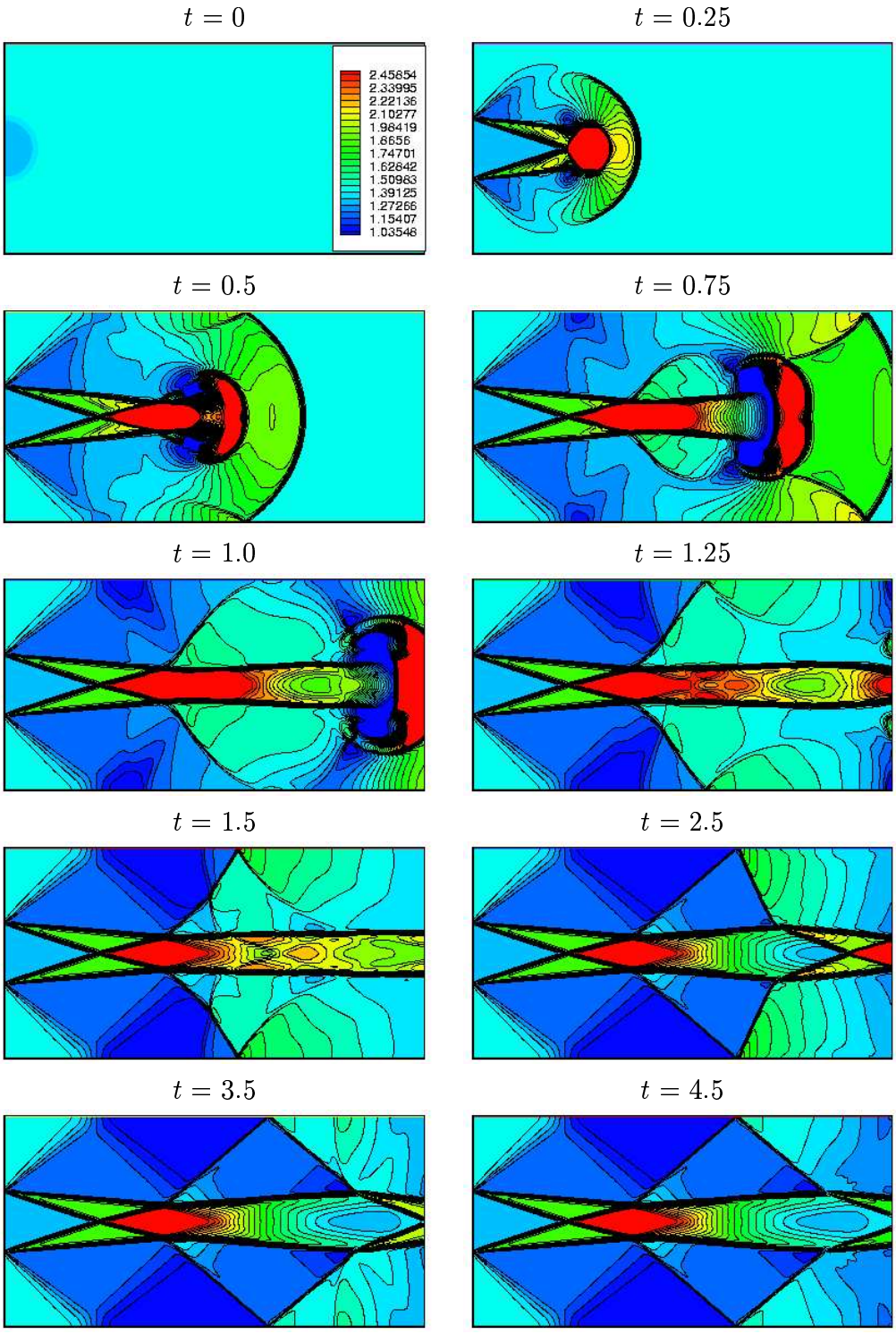
$t = 0$
2.45854
2.33995
2.22136
2.10277
1.98419
1.8656
1.74701
1.62842
1.50983
1.39125
1.27266
1.15407
1.03548
$t = 0.25$
$t = 0.5$
$t = 0.75$
$t = 1.0$
$t = 1.25$
$t = 1.5$
$t = 2.5$
$t = 3.5$
$t = 4.5$

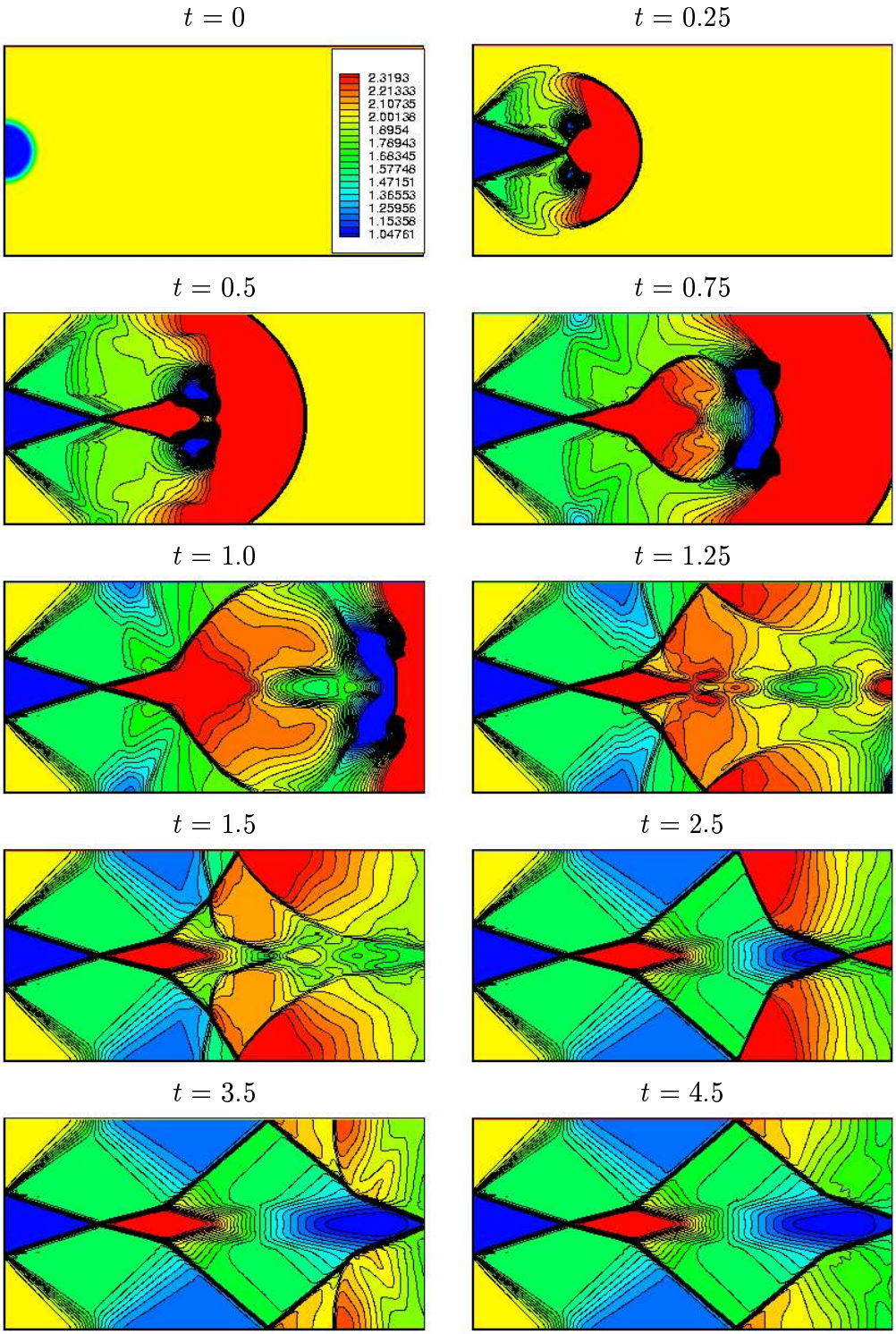

Figure 5: Supersonic overexpanded jet at different time levels. First, second and third series: ratio of specific heats, density and pressure, respectively. Pressure of ambient air is 2 times higher than the exhaust pressure. The grid has 400×200 cells and $\Delta t = 1.25 \times 10^{-4} \Delta x$.

with similar methods. The results do not suffer from pressure oscillations near the two-fluid interfaces.

REFERENCES

[1] R. Abgrall and S. Karni. Computations of compressible multifluids. *J. Comp. Phys.* **169**, 594–623, (2001).

[2] B. Cockburn and C.W. Shu. TVB Runge-Kutta local projection discontinuous Galerkin finite element method for conservation laws II: general framework. *Math. Comp.* **52**, 411–435, (1989).

[3] B. Cockburn, S. Lin and C.W. Shu. TVB Runge-Kutta local projection discontinuous Galerkin finite element method for conservation laws III: one-dimensional systems. *J. Comp. Phys.* **84**, 90–113, (1989).

[4] B. Cockburn, S. Hou and C.W. Shu. The Runge-Kutta local projection discontinuous Galerkin finite element method for conservation laws IV: the multidimensional case. *Math. Comp.* **54**, 545–581, (1990).

[5] B. Cockburn and C.W. Shu. The Runge-Kutta discontinuous Galerkin method for conservation laws V: multidimensional systems. *J. Comp. Phys.* **141**, 199–224, (1998).

[6] R.P. Fedkiw, T. Aslam, B. Merriman and S. Osher. A non-oscillatory Eulerian approach to interfaces in multimaterial flows. *J. Comp. Phys.* **152**, 457–492, (1999).

[7] J.F. Haas and B. Sturtevant. Interaction of weak shock waves with cylindrical and spherical gas inhomogeneities. *J. Fluid Mech.* **81**, 41–76, (1987).

[8] S. Karni. Multicomponent flow calculations by a consistent primitive algorithm. *J. Comp. Phys.* **112**, p31–43, (1994).

[9] S. Karni. Hybrid multifluid algorithms. *SIAM J. Sci. Comp.* **17**, 1019–1039, (1996).

[10] B. Koren, M.R. Lewis, E.H. van Brummelen and B. van Leer. Riemann-problem and level-set approaches for homentropic two-fluid flow computations, *J. Comp. Phys.* **181**, 654–674 (2002).

[11] B. Koren. A robust upwind discretization method for advection, diffusion and source terms, in: *Numerical Methods for Advection-Diffusion Problems* (C.B. Vreugdenhil and B. Koren, eds.). *Notes on Numerical Fluid Mechanics*, **45**, 117-138, Vieweg, Braunschweig (1993).

[12] B. van Leer. Towards the ultimate conservation difference scheme, II. *J. Comp. Phys.* **14**, 361–376, (1974).

[13] B. van Leer. Towards the ultimate conservation difference scheme, V. *J. Comp. Phys.* **32**, 1–136, (1979).

[14] G.H. Markstein. Chapter B: Theory of Flame Propagation, in: *Non-Steady Flame Propagation* (G.H. Markstein, ed.), 5–14, Pergamon Press, New York, (1964).

[15] W.A. Mulder, S. Osher and J.A. Sethian. Computing interface motion in compressible gas dynamics. *J. Comp. Phys.* **100**, 209–228, (1992).

[16] J. Naber. *A Runge-Kutta discontinuous-Galerkin level-set method for unsteady compressible two-fluid flow*, Report MAS-E0601, CWI, http://ftp.cwi.nl/CWIreports/MAS/MAS-E0601.pdf, Amsterdam, (2006).

[17] S. Osher and J.A. Sethian. Fronts propagating with curvature-dependent speed: algorithms based on Hamilton-Jacobi formulations. *J. Comp. Phys.* **79**, 12–49, (1988).

[18] J.J. Quirk and S. Karni. *On the dynamics of a shock-bubble interaction.* ICASE Report 94-75, Institute for Computer Applications in Science and Engineering, NASA Langley Research Center, Hampton, VA, (1994).

[19] M. Sussman and E. Fatemi. An efficient, interface-preserving level set redistancing algorithm and its application to interfacial incompressible fluid flow. *SIAM J. Scient. Comp.* **20**, 1165–1191, (1999).

[20] M. Sussman, P. Smereka and S. Osher. A level-set approach for computing solutions to incompressible two-phase flow. *J. Comp. Phys.* **114**, 146-159, (1994).

[21] J. Wackers and B. Koren. A fully conservative model for compressible two-fluid flow, *Int. J. Num. Meth. Fluids* **47**, 1337–1343, (2005).